

# Folding Studies on the Human Chorionic Gonadotropin $\beta$ -Subunit Using Optical Spectroscopy of Peptide Fragments

R. A. Gangani D. Silva,<sup>†</sup> Simon A. Sherman,<sup>‡</sup> Fulvio Perini,<sup>\*,§</sup> Elliott Bedows,<sup>\*,§,||</sup> and Timothy A. Keiderling<sup>\*,†</sup>

Contribution from the Department of Chemistry (M/C 111), University of Illinois at Chicago, 845 W. Taylor Street, Chicago, Illinois 60607-7061, the Eppley Institute for Research in Cancer and Allied Diseases, University of Nebraska Medical Center, 986805 Nebraska Medical Center, Omaha, Nebraska 68198-6805, The Department of Biochemistry and Molecular Biology, University of Nebraska Medical Center, 986805 Nebraska Medical Center, Omaha, Nebraska 68198-6805, and The Department of Pharmacology, University of Nebraska Medical Center, 986805 Nebraska Medical Center, Omaha, Nebraska 68198-6805

Received April 14, 2000

**Abstract:** Conformational preferences for the peptides SRPINATLAVEKEGSPVSITVNTTISA (H1) and APTMTRVLQGVLPALPQVVCNYR (H2) corresponding to the amino acid residues 9–35 and 38–60, respectively, of the glycoprotein hormone human chorionic gonadotropin  $\beta$ -subunit (hCG $\beta$ ) were studied by Fourier transform infrared spectroscopy (FTIR) and vibrational and electronic circular dichroism (VCD and ECD) in various environments. These peptides correspond to the H1 ( $\beta$ -like) and H2 (loop) hairpins of the native-state hCG $\beta$  subunit defined by X-ray analysis. As demonstrated by FTIR and VCD, the H1 peptide adopts a  $\beta$ -structure in water as well as in environments that normally induce  $\alpha$ -helix formation, such as mixed trifluoroethanol/H<sub>2</sub>O solvent or micellar concentrations of sodium dodecyl sulfate. By contrast, the H2 peptide ECD and VCD spectra are consistent with a significant fraction of the residues being in either a poly-L-proline II like or a partially helical conformation depending on the environment. A third peptide, H3, corresponding to the 60–87 hairpin region of hCG $\beta$ , which was studied previously, switches its conformation depending on both the solvent and peptide concentration. Taken together, the data suggest that hCG $\beta$  may fold by, first, the H1 region rapidly adopting a  $\beta$ -hairpin structure, followed by its hydrophobic collapse with the H3 region, which in turn facilitates the formation of the H3  $\beta$ -hairpin. The H2 hairpin loop is formed as a result of the formation of the H1 and H3  $\beta$ -hairpin interactions.

## Introduction

Human chorionic gonadotropin (hCG) is a glycoprotein hormone. All members of the glycoprotein hormone family are noncovalently bound heterodimeric proteins that share a common  $\alpha$ -subunit and have differing  $\beta$ -subunits that confer biological specificity.<sup>1</sup> The normal physiological function of hCG is to maintain pregnancy by inducing the secretion of progesterone by the corpus luteum of the ovary. However, both hCG and, more frequently, the free (unassembled) hCG $\beta$  subunit are expressed and secreted as tumor markers in a variety of cancers.<sup>2,3</sup>

The X-ray crystallographic structure for hCG has been reported.<sup>4,5</sup> The crystalline structure of hCG $\beta$  consists of three hairpin-like segments (see Figure 1), two of which (H1 and H3)

are antiparallel  $\beta$ -sheet-like hairpins, whereas the other (H2) is an extended hairpin-like segment that does not have a regular series of hydrogen bonds between the two strands forming the H2 loop. The  $\alpha$ - and  $\beta$ -subunits of hCG are stabilized by a “seat belt” formed by hCG $\beta$  residues 100–110.<sup>4</sup> The intracellular folding pathway of hCG $\beta$  has been defined using disulfide bond formation to monitor subunit folding.<sup>6–9</sup>

Previous hCG $\beta$  folding studies were conducted in an intracellular environment where folding events were studied on the minute time scale. To understand the nucleation events that initiate the early stages of the hCG $\beta$  folding, in this paper we spectroscopically studied the structural properties of three peptides corresponding to the H1, H2, and H3 hairpin loops of the hCG $\beta$  subunit (Figure 1). Studies of relevant peptide sequences derived from proteins have been previously used to

\* To whom correspondence should be addressed. Phone (312) 996-3156. Fax: (312) 996-0431. E-mail: tak@uic.edu.

<sup>†</sup> University of Illinois at Chicago.

<sup>‡</sup> Eppley Institute for Research in Cancer and Allied Diseases, University of Nebraska Medical Center.

<sup>§</sup> The Department of Biochemistry and Molecular Biology, University of Nebraska Medical Center.

<sup>||</sup> The Department of Pharmacology, University of Nebraska Medical Center.

(1) Pierce, J. G.; Parsons, T. F. *Annu. Rev. Biochem.* **1981**, *50*, 465–495.

(2) Ruddon, R. W.; Norton, S. E. *Semin. Oncol.* **1993**, *20*, 251–260.

(3) Bedows, E.; Norton, S. E.; Huth, J. R.; Ruddon, R. W., *J. Biol. Chem.* **1994**, *269*, 10574–10580.

(4) Laphorn, A. J.; Harris, D. C.; Littlejohn, A.; Lustbader, J. W.; Canfield, R. E.; Machin, K. J.; Morgen, F. J.; Isaacs, N. W. *Nature* **1994**, *369*, 455–461.

(5) Wu, H.; Lustbader, J. W.; Liu, Y.; Canfield, R. E.; Hendrickson, W. A. *Structure* **1994**, *2*, 545–558.

(6) Huth, J. R.; Mountjoy, K.; Perini, F.; Ruddon, R. W. *J. Biol. Chem.* **1992**, *267*, 8870–8879.

(7) Bedows, E.; Huth, J. R.; Ruddon, R. W. *J. Biol. Chem.* **1992**, *267*, 8880–8886.

(8) Bedows, E.; Huth, J. R.; Sukanuma, N.; Bartels, C.; Boime, I.; Ruddon, R. W. *J. Biol. Chem.* **1993**, *268*, 11655–11662.

(9) Beebe, J. S.; Mountjoy, K.; Krzesicki, R. F.; Perini, F.; Ruddon, R. W. *J. Biol. Chem.* **1990**, *265*, 312–317.

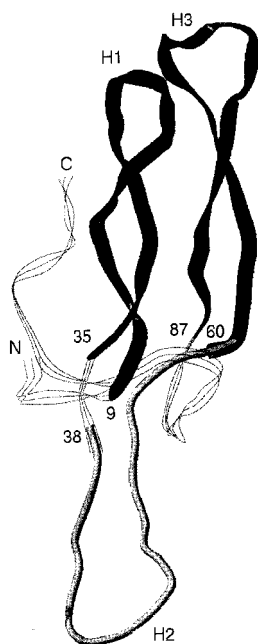


**Figure 1.** Ribbon diagram of the X-ray crystal structure of the hCG $\beta$  protein subunit as downloaded from the protein data bank. The H1, H2, and H3 hairpins are noted on the schematic.

understand the nucleation events that can initiate the early stages of protein folding.<sup>10–16</sup> This approach can also provide an understanding of the propensities to form specific secondary structures for various amino acid sequences (protein fragments) of interest. Peptide studies can also help distinguish whether a hydrophobic collapse or a framework folding mechanism best describes the early folding events of the corresponding protein.<sup>17</sup> Furthermore, by changing the peptide environment (for example, by adding sodium dodecyl sulfate (SDS) or trifluoroethanol (TFE)), the effect of dehydration can be simulated to approximate that which would be found in membrane and/or protein interior environments. Comparison of data from perturbed peptide systems with data obtained for the peptide in water or buffer can then lead to further understanding of intrinsic folding propensities under equilibrium conditions.

Spectroscopic methods have long had an important role in the structural determination of biological molecules. In this work we use a combination of three complementary methods. The first is electronic circular dichroism (ECD) that in the UV yields a good measure of  $\alpha$ -helix formation and provides an indication of other secondary structure formation. ECD requires only a small amount of material, can be used to study molecules in many solvents, and is a quick, nondestructive method.<sup>18–20</sup> On the other hand, broad overlapped bands and side chain contribu-

tions<sup>21,22</sup> can make ECD spectra less interpretable. The second method, infrared (IR) spectroscopy, has grown in use over the past decade for determination of structural features of proteins and peptides in environments that cannot be studied with other methods.<sup>23–25</sup> IR spectroscopy can be very useful in distinguishing  $\beta$ -structure in solution from helical and unordered conformations but is less helpful in distinguishing helical from unordered conformations. Finally, vibrational circular dichroism (VCD) combines the advantages of IR and ECD by coupling the resolution of vibrational spectra to the stereochemical sensitivity of circular dichroism.<sup>26–31</sup> Since each technique has its own advantages and disadvantages, when they are used in combination, the ambiguities that might arise by using only one technique can be overcome.

The optical spectra for these peptides were studied in different solvent environments at various concentrations and temperatures. Such environmental perturbations were used to probe the peptides' intrinsic propensities to form particular secondary structures. On the basis of the H1 and H2 peptide results reported here, in combination with earlier results for the H3 peptide,<sup>32</sup> we propose a novel mechanism for hCG $\beta$  subunit folding.

## Materials and Methods

The H2 peptide (APTMTRVLQGVLPALPQVVCNYR, hCG<sub>38–60</sub>, with a Cys to Ala mutation at the N terminus, position 38) was synthesized at the Eppley Cancer Institute Molecular Biology Core Facility as described earlier.<sup>33</sup> The H1 peptide (SRPINATLAVEKEGSPVSITVNTTISA, hCG<sub>9–35</sub>, with Cys to Ser mutations at positions 9, 23, 26, and 34) was synthesized by AnaSpec Inc. (San Jose, CA) and purified at the Eppley Cancer Institute. These amino acid substitutions were used to avoid artifactual disulfide bond formation and aggregation. Characterization of the peptides and confirmation of their sequences was done by amino acid analysis, HPLC, and mass spectrometry.

D<sub>2</sub>O was purchased from Cambridge Isotope Laboratories. Doubly distilled water was used in the ECD experiments. Spectral grade TFE from Aldrich was used without further purification. Deuterated TFE-OD was prepared in the lab by mixing TFE with D<sub>2</sub>O (~1:30 v/v) and distilling. TFE-OD was collected at 78 °C and then redistilled 2–3 more times from fresh D<sub>2</sub>O. SDS was purchased from Sigma-Aldrich.

**Electronic CD.** The ECD spectra for both peptides, H1 and H2, were measured in pure water and various mixtures of TFE/H<sub>2</sub>O and

(20) Venyaminov, S. Y.; Yang, J. T. In *Circular Dichroism and the Conformational Analysis of Biomolecules*; Fasman, G. D., Ed.; Plenum Press: New York, 1996; pp 69–107.

(21) Krittanaï, C.; Johnson, W. C. *Anal. Biochem.* **1997**, *253*, 57–64.

(22) Woody, R. W.; Dunker, A. K. In *Circular Dichroism and the Conformational Analysis of Biomolecules*; Fasman, G. D., Ed.; Plenum Press: New York, 1996; pp 109–157.

(23) Mantsch, H. H.; Chapman, D. *Infrared Spectroscopy of Biomolecules*; Wiley-Liss: Chichester, U.K., 1996.

(24) Goormaghtigh, E.; Cabiaux, V.; Ruysschaert, J. M. In *Subcellular Biochemistry*; Hilderson, H. J., Ralston, G. B., Eds.; Plenum: New York, 1994; Vol. 23, pp 329–362.

(25) Arrondo, J. L. R.; Muga, A.; Castresana, J.; Goni, F. M. *Prog. Biophys. Mol. Biol.* **1992**, *59*, 23–56.

(26) Freedman, T. B.; Nafie, L. A.; Keiderling, T. A. *Biopolymers* **1995**, *37*, 265–279.

(27) Nafie, L. A. *Annu. Rev. Phys. Chem.* **1997**, *48*, 357–386.

(28) Diem, M. In *Biomolecular Spectroscopy II*; Birge, R. R., Nafie, L. A., Eds.; SPIE, 1991; pp 28–36.

(29) Keiderling, T. A.; Silva, R. A. G. D.; Yoder, G.; Dukor, R., K. *Bioorg. Med. Chem.* **1999**, *7*, 133–141.

(30) Keiderling, T. A. In *Circular Dichroism and the Conformational Analysis of Biomolecules*; Fasman, G. D., Ed.; Plenum: New York, 1996; pp 555–598.

(31) Keiderling, T. A. In *Circular dichroism: principles and applications for chemists and biologists*, 2nd ed.; Nakanishi, K., Berova, N., Woody, R. A., Eds.; John Wiley & Sons: New York, 2000; pp 621–666.

(32) Silva, R. A. G. D.; Sherman, S. A.; Keiderling, T. A. *Biopolymers* **1999**, *50*, 413.

(33) Sherman, S. A.; Gmeiner, W. H.; Kimarskiy, L.; Perini, F.; Ruddon, R. W. *J. Biomol. Struct. Dyn.* **1995**, *13*, 441–445.

(10) Viguera, A. R.; Jimenez, M. A.; Rico, M.; Serrano, L. *J. Mol. Biol.* **1996**, *255*, 507–521.

(11) Ramirez-Alvarado, M.; Serrano, L.; Blanco, F. J. *Protein Sci.* **1997**, *6*, 162–174.

(12) Prieto, J.; Wilmans, M.; Jimenez, M. A.; Rico, M.; Serrano, L. *J. Mol. Biol.* **1997**, *268*, 760–778.

(13) Yang, J. J.; Buck, M.; Pitkeathly, M.; Kotik, M.; Haynie, D. T.; Dobson, C. M.; Radford, S. E. *J. Mol. Biol.* **1995**, *253*, 483–491.

(14) Yang, J. J.; Van den Berg, B.; Pitkeathly, M.; Smith, L. J.; Bolin, K. A.; Keiderling, T. A.; Redfield, C.; Dobson, C. M.; Radford, S. E. *Folding Des.* **1996**, *1*, 473–484.

(15) Neira, J. L.; Rico, M. *Folding Des.* **1997**, *2*, R1–R11.

(16) Reymond, M. T.; Merutka, G.; Dyson, H. J.; Wright, P. E. *Protein Sci.* **1997**, *6*, 706–716.

(17) Baldwin, R. L. *J. Biomol. NMR* **1995**, *5*, 103–109.

(18) Johnson, W. C. *Proteins* **1990**, *7*, 205–214.

(19) Johnson, W. C. *Methodol. Enzymol.* **1992**, *210*, 426–447.

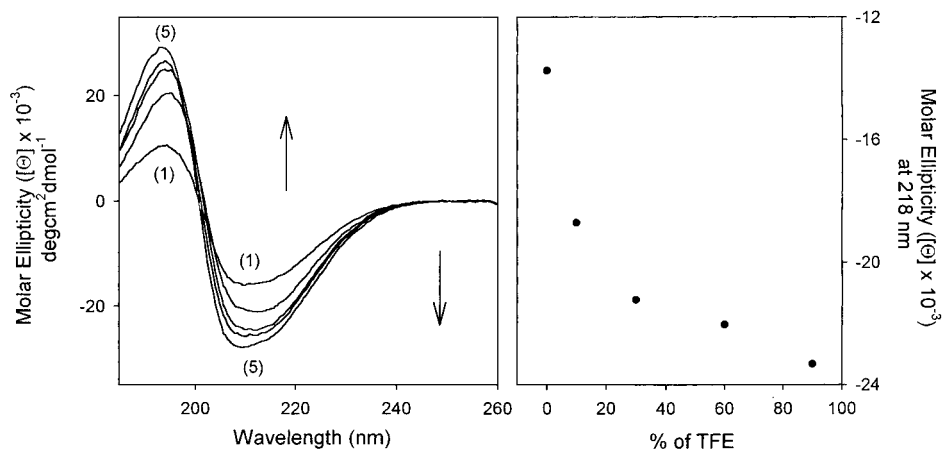


**Figure 2.** Normalized ECD spectra obtained for a TFE titration of the H1 peptide (left). The peptide concentration was 0.1 mg/mL, and the cell path length was 1 mm. The percentages of TFE present in the solvents were: (1) 0, (2) 10, (3) 30, (4) 60, and (5) 90, respectively. Spectra are expressed as molar ellipticity per residue units after subtracting relevant baselines recorded for solvent in the same cell. A plot of molar ellipticity of each spectrum at 218 nm vs the amount of TFE present in the solvent is given (right).

SDS/H<sub>2</sub>O. The spectra were recorded over the 260–185 nm region using a JASCO model J-600 spectrometer, upgraded with JASCO Windows-based software. Concentrations of the samples ranged from 0.1 mg/mL (1 mm path length cell) to 1 mg/mL (50  $\mu\text{m}$  path length cell). Spectra were obtained as the average of 8–10 scans with a time constant of 2 s. Relevant baselines were obtained by measuring just the solvent in the same cells and were subtracted from the corresponding sample spectra. The resultant spectra were re-expressed in terms of molar ellipticity,  $[\theta]$  ( $\text{deg cm}^2 \text{ dmol}^{-1}$ ), on a per residue basis.

**Vibrational CD.** VCD spectra and (low-resolution) IR absorption under identical conditions were measured using a dispersive instrument at the University of Illinois at Chicago (UIC). The construction and the use of this instrument for studying biomolecules have been previously described in detail.<sup>31,34</sup> The VCD spectra have a 10  $\text{cm}^{-1}$  resolution, were collected with a 10 s time constant, and are an average of six scans. Baselines of pure solvent or mixed solvent systems, as appropriate, were measured using the same cells and subtracted from the sample spectra. Sample VCD spectra were rescaled (to  $A = 1$ ) using the absorbance of the amide I' band for easy comparison with other peptide VCD spectra. The VCD instrument was checked regularly for artifacts by measuring optically inactive compounds such as poly-DL-lysine or trifluoroacetic acid and for possible frequency shifts by measuring the known VCD spectra of poly-L-lysine.

**FTIR.** The same samples used to record VCD spectra were used to record FTIR spectra with higher resolution and improved S/N. These measurements were done with a BioRad FTS-60A spectrometer, at 4  $\text{cm}^{-1}$  resolution, as an average of 1024 scans in the mid-IR region. Final FTIR spectra were obtained after subtraction of the background solvent and water vapor spectra from the sample spectra. In some cases the FTIR spectra were subjected to Fourier self-deconvolution (FSD)<sup>35</sup> using a variety of deconvolution parameters, and the best results were selected. Methods used for sample preparation and the cleaning and filling of the cells have been described previously.<sup>31,32</sup>

## Results

**Studies on the H1 Peptide.** The H1 peptide (Figure 1, hairpin 1) in water with 0.1 mg/mL concentration had an ECD spectrum with a band shape and intensity (Figure 2, spectrum 1) consistent with those of a  $\beta$ -structure, having a minimum at  $\sim 212$  nm and a maximum at  $\sim 195$  nm.<sup>36,37</sup> That the H1 peptide had a significant  $\beta$ -structure content was confirmed by IR as well as

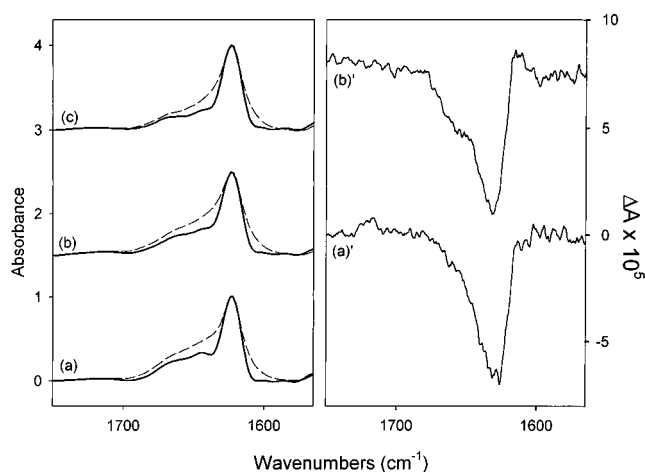


**Figure 3.** Rescaled (to  $A = 1$ ) FTIR absorbance spectra (left) of the H1 peptide amide I' in three different solvent environments. In all three experiments, a 50  $\mu\text{m}$  path length was used with peptide concentrations of 16–21 mg/mL. Spectra were deconvoluted<sup>35</sup> using  $\gamma = 11$  and a filter function of 68 and are plotted with “thick lines” underneath corresponding normal absorbance spectra “dashed thin lines”. VCD spectra (right) were measured of the same samples (in D<sub>2</sub>O and SDS only) in the same cells used to record FTIR (left) and rescaled to an amide I' peak absorbance of 1 using the dispersive IR absorbance spectra (not shown). Solvents used: (a, a') D<sub>2</sub>O, (b, b') 250 mM SDS, and (c) 80% TFEOD.

VCD spectral analyses, which were recorded at a higher peptide concentration (21 mg/mL) in D<sub>2</sub>O. The FTIR spectrum had its major amide I' band at  $\sim 1622$   $\text{cm}^{-1}$  with the presence of weaker additional component bands in the 1640–1660  $\text{cm}^{-1}$  region (Figure 3, left, spectrum a), presumably arising from unordered segments of the peptide. These additional features could be more clearly seen following deconvolution (FSD) as shown in the trace beneath the original spectrum. The VCD spectrum of the H1 peptide, recorded with the same sample used for the FTIR, consisted of a negative band centered at  $\sim 1620$   $\text{cm}^{-1}$ , with a broad component to higher frequency (Figure 3, right, spectrum a'). This is similarly consistent with a  $\beta$ -dashed conformation having some disordered component.

To test for the monomeric nature of the H1 peptide, FTIR as well as ECD measurements were carried out on a series of more dilute samples prepared by reducing the concentration of the peptide from 21 mg/mL (7.8 mM) to 0.2 mg/mL (73  $\mu\text{M}$ ) in D<sub>2</sub>O for the IR and from 1 mg/mL (0.37 mM) to 0.0025 mg/

(34) Keiderling, T. A. In *Practical Fourier Transform Infrared Spectroscopy*; Krishnan, K., Ferraro, J. R., Eds.; Academic Press: San Diego, 1990; pp 203–284.

(35) Griffiths, P. R.; Pariente, G. L. *Trends Anal. Chem.* **1986**, 5, 209–215.

(36) Greenfield, N.; Fasman, G. D. *Biochemistry* **1969**, 8, 4108–4116.

(37) Greenfield, N. J. *Anal. Biochem.* **1996**, 235, 1–10.

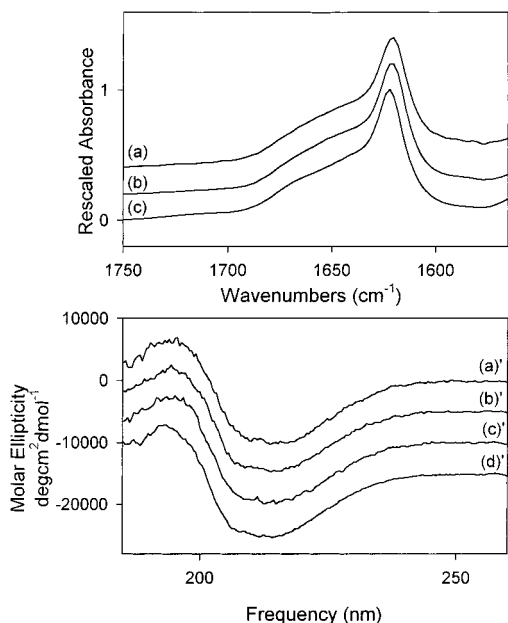


**Figure 4.** Rescaled FTIR absorbance spectra (top) of the H1 peptide with concentrations of (a) 21 mg/mL, (b) 0.83 mg/mL, and (c) 0.21 mg/mL peptide in D<sub>2</sub>O. Path lengths of 50  $\mu$ m for (a) and 100  $\mu$ m for (b) and (c) were used. ECD spectra (bottom) of the H1 peptide with concentrations of (a) 1 mg/mL, (b) 0.1 mg/mL, (c) 0.01 mg/mL, and (d) 0.0025 mg/mL in H<sub>2</sub>O. Path lengths of 0.1 mm for (a), 1 mm for (b), and 10 mm for (c) and (d) were used, respectively.

mL (0.73  $\mu$ M) in H<sub>2</sub>O for ECD. The results obtained (Figure 4) were all consistent in terms of spectral band shape and component frequencies over this 100-fold IR and 400-fold ECD dilution range. This confirmed that the conformation of the H1 peptide in water is not changed over this concentration range and implies that the peptide is monomeric in aqueous solution. The  $\beta$ -conformation adopted by the H1 peptide (0.1 mg/mL) in water was stable from 4 to 50 °C. There was, however, a small decrease in intensity of the ECD spectra recorded at temperatures above 50 °C (at 55 and 60 °C). On cooling, the original spectrum of the peptide at 4 °C was almost fully recoverable (data not shown).

Studies of the H1 peptide in helix-promoting environments, such as TFE/H<sub>2</sub>O mixtures and micellar SDS, were used to test the resistance of the H1 peptide to changes in its  $\beta$ -conformation. The FTIR spectra of the H1 peptide at a 16 mg/mL concentration in 80% TFE-OD were again characteristic of peptides with a  $\beta$ -conformation (Figure 3) as were the corresponding VCD spectra (data not shown). The ECD spectrum of the H1 peptide (0.1 mg/mL), when titrated with TFE, also suggested that the  $\beta$ -conformation of the peptide was maintained in the presence of solvent, although these ECD band shapes are somewhat distorted and the intensity does rise with increasing TFE fraction (Figure 2). The latter might suggest the presence of a small helical component within the H1 peptide under these conditions.

FTIR and VCD spectra of the H1 peptide (19 mg/mL) in micellar SDS (250 mM) show that the  $\beta$ -conformation is predominant in this environment as well (Figure 3). The ECD spectra of the H1 peptide (1 mg/mL) in increasing concentrations of SDS, ranging from 0.6 to 107 mM, indicate that the H1 peptide maintains a significant fraction of  $\beta$ -structure in all SDS-containing environments tested. However, the ECD spectra did dramatically change in intensity (Figure 5, right) and experienced some frequency shift (Figure 5, left) as the SDS concentration changed. In the presence of 0.6 mM SDS, the ECD spectral intensity of the H1 peptide decreased by about a

factor of 2 compared to that of the spectrum recorded in water. In addition, the spectral minimum shifts from  $\sim$ 215 to  $\sim$ 218 nm. In concentrations of up to  $\sim$ 2.5 mM SDS, the H1 peptide ECD intensity continually weakened and shifted to longer wavelength,  $\sim$ 222 nm. A sharp transition can be seen at  $\sim$ 2.5 mM SDS (Figure 5, left), after which the ECD intensity of the H1 peptide became more intense and the minima shifted back again toward shorter wavelengths. All FTIR spectra recorded for 10 mg/mL H1 peptide concentrations in D<sub>2</sub>O with varying amounts of SDS (0, 2.5, 5, and 10 mM) had absorbance maxima at  $\sim$ 1622  $\text{cm}^{-1}$  and, hence, did not show any frequency shifts. However, a small difference in band shape was seen in the spectrum recorded for H1 in just D<sub>2</sub>O as compared to the spectra for the peptide in SDS solution (results not shown). ECD measurements of the H1 peptide (0.1 mg/mL peptide in 6 mM SDS and 0.1 mg/mL in 0.6 mM SDS) taken over 6 days did not show any conformational changes from  $\beta$ -structures except for small, random fluctuations (data not shown).

**Studies on the H2 Peptide.** The ECD spectra of the H2 peptide (0.1 mg/mL, in H<sub>2</sub>O) suggested a conformation dominated by unordered components as indicated by a spectrum with a broad negative feature at  $\sim$ 198 nm (Figure 6, spectrum 1). This peptide was previously studied by NMR, which indicated that, in H<sub>2</sub>O, most of the amino acid residues within the H2 peptide adopt a poly-L-proline II (PLPII) like conformation.<sup>33</sup> With increasing temperature, the ECD spectra of this peptide displayed a change in band shape with decreased negative intensity (compared to the 5 °C spectrum) at shorter wavelengths than 200 nm and increased negative intensity at  $\sim$ 220 nm. This suggested that either a small gain of helix or sheet structure or a loss of PLPII-like structure occurred with an increase in temperature (data not shown). Upon cooling, the starting spectrum was recovered completely at 5 °C. FTIR and VCD spectra of the H2 peptide at higher concentrations were also consistent with the H2 peptide having an unordered structure. The amide I' absorbance at  $\sim$ 1644  $\text{cm}^{-1}$  (Figure 7, spectrum a) and its negative couplet VCD, with the negative band centered at  $\sim$ 1630  $\text{cm}^{-1}$  (Figure 7, spectrum a'), are typical of a random coil. Consistent with the interpretation of NMR data for the H2 peptide,<sup>33</sup> the VCD spectrum in D<sub>2</sub>O was also consistent with a PLPII-like form (left-handed extended helix).<sup>29,38</sup>

The H2 peptide was studied in different environments to probe its propensity to adopt other structures. ECD experiments with increasing percentages of TFE in the solvent indicated that the H2 peptide (0.1 mg/mL) underwent a gradual transition from an unordered to a partially helical conformation in a process characterized by a near isodichroic point (Figure 6). At higher percentages of TFE, the spectral band shape remained roughly the same whereas the intensity steadily increased. High-concentration FTIR and VCD experiments in 20% and 50% TFE-OD environments showed VCD spectra indicative of a progressive change from unordered to a mixed helix/coil conformation (Figure 7). IR spectra of the H2 peptide in TFE-OD still had amide I' maxima in the typical region for unordered bands, but shifted up slightly to 1646  $\text{cm}^{-1}$ . Consistent with this, the VCD spectrum in 20% TFE-OD showed only a reduction in intensity of the band shape associated with a coil. This probably resulted from a cancellation of the coil contribution to the spectrum that would accompany the growth of a helical component. By contrast, the spectrum recorded in 50% TFE-OD was a spectrum typical of a helix/coil mixed structure. (The VCD spectral signature for a helix is a positive couplet and thus has a spectral signature opposite in sign that

(38) Dukor, R. K.; Keiderling, T. A. *Biopolymers* **1991**, *31*, 1747–1761.

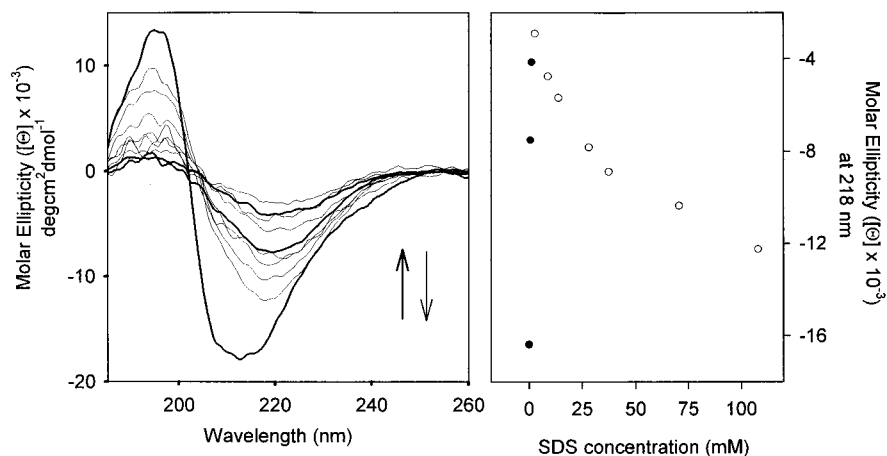


**Figure 5.** ECD spectra (left) corresponding to an SDS titration of the H1 peptide obtained with a peptide concentration of 1 mg/mL and a path length of 50  $\mu\text{m}$ . The concentrations of SDS were (1) 0.0, (2) 0.6, and (3) 1.2 mM (thick lines) and (4) 2.7, (5) 8.9, (6) 13.8, (7) 28.1, (8) 37.4, (9) 70.5, and (10) 108.0 mM (thin lines). Baselines were measured in the same cell with just  $\text{H}_2\text{O}$ . The molar ellipticity at 218 nm is plotted (right) vs the SDS concentration (mM) for each sample. Values corresponding to SDS concentration up to 1.2 mM are represented by filled circles, whereas those corresponding to higher concentrations of SDS are given as empty circles.

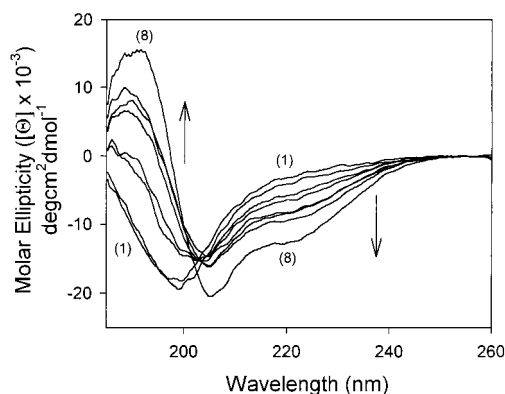


**Figure 6.** Normalized ECD spectra corresponding to the TFE titration of the H2 peptide obtained with 0.1 mg/mL peptide in a 1 mm path cell. Baseline correction and rescaling were as for Figure 2. Percentages of TFE changed from 0 (1) to 10 (2), 20 (3), 30 (4), 40 (5), 50 (6), 60 (7), and 90 (8), respectively.

tends to cancel the random coil VCD spectra in mixed structures.<sup>29,39</sup>

SDS-induced perturbations on the H2 peptide paralleled those seen with TFE. In nonmicellar SDS environments, which can be  $\beta$ -structure-promoting,<sup>40,41</sup> the ECD spectra of the H2 peptide (1 mg/mL) instead showed a partial helical spectral signature (Figure 8). The VCD spectra again showed a gain of  $\alpha$ -helix fraction and a loss of unordered fraction in SDS such as described above for TFE. Consistent with this, the FTIR band shifted toward a higher wavenumber (Figure 9). Thus, similar partial helix formation was found in both nonmicellar and micellar SDS for the H2 peptide. By contrast, the other two peptides studied, H1 (above) and H3,<sup>32</sup> adopted a  $\beta$ -structure in a (nonmicellar) SDS environment.

## Discussion

We have demonstrated that the three peptides H1, H2, and H3, corresponding to three different hairpin loops in the X-ray

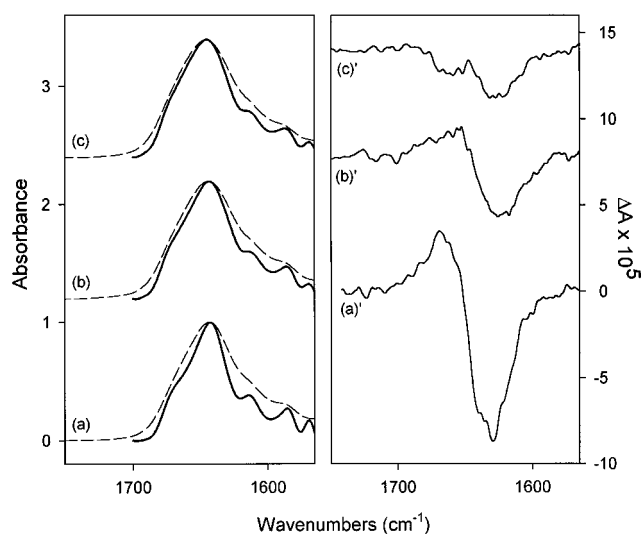


**Figure 7.** Rescaled FTIR spectra (left, dashed thin lines) and VCD spectra (right) of the H2 peptide recorded in (a, a')  $\text{D}_2\text{O}$ , (b, b') 20% TFE-OD, and (c, c') 50% TFE-OD. The sample concentration in each case was 25 mg/mL, and the path length was 50  $\mu\text{m}$ . These FTIR spectra were FSD deconvoluted (thick lines), and VCD spectra were rescaled as in Figure 3.

structure of the hCG $\beta$  subunit, have different intrinsic propensities toward adopting particular secondary structures. These were distinguished by combining complementary optical spectroscopic data from ECD, IR, and VCD.

In some previous studies of peptide sequences derived from proteins containing mainly  $\beta$ -structure, typically by NMR, a well-defined secondary structure was not found in water.<sup>10,42,43</sup> Such peptides are usually described as being unstructured when isolated in aqueous solution. This suggests that tertiary interactions play a major role in allowing such peptides to form secondary structure in the parent protein native state. Our H2 data follow this pattern, revealing no clear secondary structural elements for the H2 peptide in water. However, there are instances where such isolated protein fragments have helical structures<sup>15,44–47</sup> or where  $\beta$ -hairpins have been identified.<sup>48–50</sup>

(39) Baumruk, V.; Huo, D. F.; Dukor, R. K.; Keiderling, T. A.; Lelievre, D.; Brack, A. *Biopolymers* **1994**, *34*, 1115–1121.

(40) Wang, L.; Voloshin, O. N.; Stasiak, A.; Camerini-Otero, R. D. *J. Mol. Biol.* **1998**, *277*, 1–11.

(41) Waterhous, D. V.; Johnson, W. C., Jr. *Biochemistry* **1994**, *33*, 2121–2128.

(42) Hamada, D.; Kuroda, Y.; Tanaka, T.; Goto, Y. *J. Mol. Biol.* **1995**, *254*, 737–746.

(43) Ramirez-Alvarado, M.; Blanco, F. J.; Niemann, H.; Serrano, L. *J. Mol. Biol.* **1997**, *273*, 898–912.

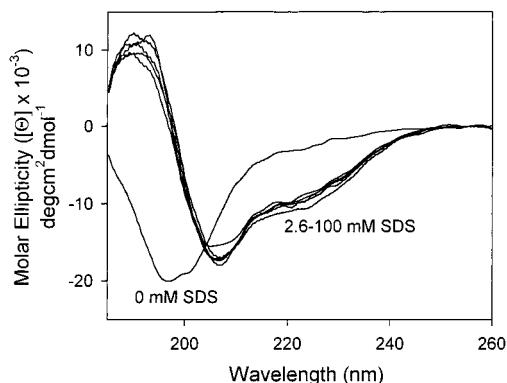


**Figure 8.** Normalized ECD spectra of the H2 peptide recorded with different amounts of SDS in the medium ranging from zero to 100 mM SDS as indicated in the figure. The peptide concentration in each case was 1 mg/mL, and the path length was 50  $\mu$ m. The baseline and rescaling were as in Figure 5.

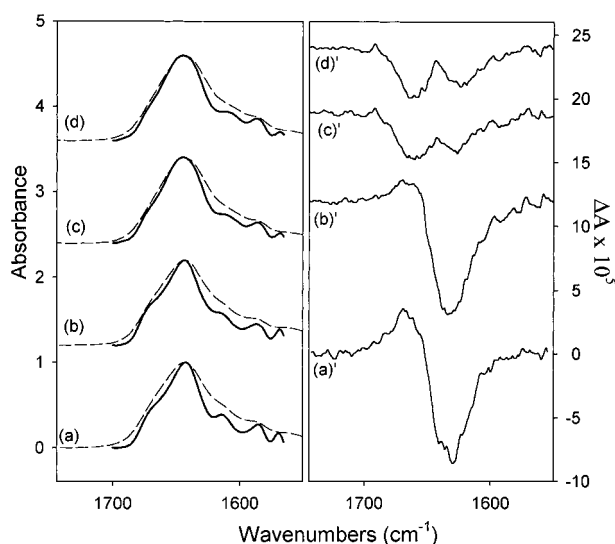


**Figure 9.** Rescaled FTIR spectra (left, dashed thin lines) recorded of the H2 peptide in (a) D<sub>2</sub>O, (b) 4.5 mM SDS, (c) 25 mM SDS, and (d) 100 mM SDS. FSD deconvolution (presented as thick lines) as in Figure 3. The peptide concentration was 25 mg/mL, and the path length was 25  $\mu$ m. VCD spectra (right) were measured on the same samples and rescaled as in Figure 3.

The H1 peptide data obtained here are consistent with the latter, more exceptional observations, providing evidence that the H1 peptide adopts a  $\beta$ -structure in water. In particular, the H1 peptide gives “normal”  $\beta$ -sheet-like ECD, FTIR, and VCD spectra and apparently does not aggregate over a fairly wide concentration range, making it a potential model for  $\beta$ -hairpin studies in the future.

**H1  $\beta$ -Hairpin Conformation.** One of the main difficulties of studying  $\beta$ -hairpins in aqueous solution is their strong tendency toward aggregation.<sup>51</sup> The frequency of the main amide

I' band at  $\sim 1622$   $\text{cm}^{-1}$  is consistent with previously suggested frequencies for a  $\beta$ -hairpin ( $\sim 1620$   $\text{cm}^{-1}$ )<sup>52</sup> and is somewhat higher than would be expected for polypeptide aggregate formation in D<sub>2</sub>O ( $\sim 1610$   $\text{cm}^{-1}$ ).<sup>53,54</sup> Also, the H1 VCD spectra are more intense than such spectra previously reported for aggregated peptides.<sup>55,56</sup> We have studied the H1 peptide at concentrations ranging over 4 orders of magnitude (0.7  $\mu$ M to 7.8 mM) in aqueous media using a combination of FTIR and ECD and have detected neither any spectral changes nor any indication of turbidity even at high sample concentrations. (We note that an exceptionally stable dimer might have these properties, but have not yet found evidence for such an interaction in aqueous H1.<sup>57</sup>) Thus, aggregation evidently did not affect our H1 peptide results, which indicates that it probably forms a monomeric, partial  $\beta$ -hairpin conformation in H<sub>2</sub>O.

The H1 peptide retains a partial  $\beta$ -conformation in nonmicellar and micellar SDS environments, but the ECD band shape and intensity did vary substantially as a function of the amount of SDS in solution. Certainly at low SDS concentrations (nonmicellar), one would expect there to be loss of the aqueous  $\beta$ -structure to account for the loss in ECD intensity. The position of the minimum of the  $\pi\pi^*$  transition in the ECD spectra can depend on the width and length of the  $\beta$ -sheet structure formed and on the characteristics of the residue side chains involved.<sup>58,59</sup> Possibly, the H1 peptide adopted  $\beta$ -structures that were of a different character in SDS than in H<sub>2</sub>O. Otherwise, it would be hard to explain the H1 peptide SDS-dependent ECD spectral band shapes and their variance from previous peptide–SDS interaction reports. (It is possible that scattering effects could reduce CD intensity in the UV;<sup>60</sup> however, absorption traces of the solvent medium indicated no significant scattering due to SDS, and the H2 (Figure 8) peptide showed no anomalous behavior in parallel SDS experiments.) For most peptides, micellar SDS promotes partial helicity, whereas nonmicellar SDS promotes  $\beta$ -structure.<sup>61</sup> Briggs et al.<sup>62</sup> have shown a signal peptide to have a  $\beta$ -structure on the surface of the membrane and  $\alpha$ -helical structure when inserted into the hydrophobic region. From the ECD intensity and frequency patterns alone, it might be tempting to speculate that nonmicellar SDS denatured the aqueous  $\beta$ -structure, resulting in loss of ECD intensity, whereas micellar SDS caused partial helical formation. However, the corresponding VCD and IR spectra very clearly indicated that a  $\beta$ -structure was dominant in water and in 250 mM SDS (Figure 3b). IR tests with intermediate SDS concentrations and with extended time in solution also supported this conclusion. By contrast, the H3 peptide, at 0.1 mg/mL in 6 mM SDS,<sup>32</sup> underwent a  $\beta$  to  $\alpha$  transition with time.

(51) Dyson, H. J.; Wright, P. E. *Annu. Rev. Biophys. Biophys. Chem.* **1991**, *20*, 519–538.

(52) Arrondo, J. L. R.; Blanco, F. J.; Serrano, L.; Goni, F. M. *FEBS Lett.* **1996**, *384*, 35–37.

(53) Surewicz, W.; Mantsch, H. H.; Chapman, D. *Biochemistry* **1993**, *32*, 389–394.

(54) Jackson, M.; Mantsch, H. H. *Crit. Rev. Biochem. Mol. Biol.* **1995**, *30*, 95–120.

(55) Yasui, S. C.; Keiderling, T. A. *J. Am. Chem. Soc.* **1986**, *108*, 5576–5581.

(56) Paterlini, M. G.; Freedman, T. B.; Nafie, L. A. *Biopolymers* **1986**, *25*, 1751–1765.

(57) Lacroix, E.; Kortemme, T.; de la Paz, M. L.; Serrano, L. *Curr. Opin. Struct. Biol.* **1999**, *9*, 487–493.

(58) Woody, R. W. *Biopolymers* **1969**, *8*, 669–683.

(59) Cantor, C. R.; Timasheff, S. N. *The Proteins*; Academic Press: New York, 1982; Vol. 5, pp 145–306.

(60) Tinoco, I.; Maestre, M. F.; Blustamante, C. *Trends Biochem. Sci.* **1983**, *8*, 41–44.

(61) Briggs, M. S.; Gierasch, L. M. *Biochemistry* **1984**, *23*, 3111–3114.

(62) Briggs, M. S.; Cornell, D. G.; Dluhy, R. A.; Gierasch, L. M. *Science* **1986**, *233*, 206–208.

(44) Brown, J. E.; Klee, W. A. *Biochemistry* **1971**, *10*, 470–476.

(45) Munoz, V.; Serrano, L.; Jimenez, M. A.; Rico, M. *J. Mol. Biol.* **1995**, *247*, 648–669.

(46) Waltho, J. P.; Feher, V. A.; Merutka, G.; Dyson, H. J.; Wright, P. E. *Biochemistry* **1993**, *32*, 6337–6347.

(47) Bruch, M. D.; Dhingra, M. M.; Gierasch, L. M. *Proteins: Struct., Funct., Genet.* **1991**, *10*, 130–139.

(48) Blanco, F. J.; Rivas, G.; Serrano, L. *Nature Struct. Biol.* **1994**, *1*, 584–590.

(49) Blanco, F. J.; Jimenez, M. A.; Herranz, J.; Rico, M.; Santoro, J.; Nieto, J. L. *J. Am. Chem. Soc.* **1993**, *115*, 5887–5888.

(50) Rico, M.; Nieto, J. L.; Santoro, J.; Bermejo, F. J.; Herranz, J. *FEBS Lett.* **1983**, *162*, 314–319.

It is important to realize that our multiple spectroscopic approach permits distinguishing among such structural possibilities. Sheet and helical structures overlap in ECD but are almost always clearly distinguished with IR or VCD. By contrast, the same sort of data for the H2 peptide indicate that it changes its conformation from one essentially unordered in H<sub>2</sub>O to one partially helical, in nonmicellar as well as micellar SDS environments. Thus, both the H1 and H2 peptides of hCG $\beta$  show unusual behavior in SDS, but in opposite ways.

To our knowledge, there are no accepted models for the promotion of  $\beta$ -structure in a peptide by addition of SDS, but there are spectroscopic reports of  $\beta$ -structure promotion of peptides in nonmicellar SDS environments.<sup>40,41</sup> In addition a previous report using pulsed-field-gradient NMR indicated the formation of a large molecular weight complex for a peptide in nonmicellar SDS environments,<sup>63</sup> which could be due to  $\beta$ -structure formation. These are much larger than the peptide: SDS ratios typical for  $\alpha$ -helix-promoting situations.<sup>64–67</sup> A model has been proposed for SDS–protein helix-forming interactions<sup>64,68</sup> in which the peptide winds around the cylindrical SDS micelle. The polypeptides would be hydrogen bonded to the sulfate heads and the hydrophobic side chains buried in the SDS tails. It was suggested that such a helix would yield spectra typical of an  $\alpha$ -helix.

Though the detailed mechanism is debatable, mixed TFE/H<sub>2</sub>O solvents are known to be helix-promoting agents for many peptides.<sup>69–74</sup> Consequently, helical conformations of peptides elucidated by the addition of TFE do not necessarily relate to any native state secondary structure.<sup>75</sup> There are a few reported cases where TFE promotes other types of secondary structures in peptides, including  $\beta$ -hairpins,<sup>76–78</sup>  $\beta$ -turns,<sup>79</sup> and 3<sub>10</sub> helices.<sup>80</sup> From our experiments, there is evidence that the H1 peptide adopts a  $\beta$ -structure in TFE/H<sub>2</sub>O mixed solvents. By contrast, the H2 peptide in the same solvents partially adopts a helical conformation, thus showing more typical structural behavior than the H1 peptide in this environment.

It has been shown that even a peptide that has a propensity to form mainly one particular type of structure can change its

**Table 1.** Major Secondary Structural Types Adopted by Peptides H1, H2, and H3 in Different Solvent Systems

environment	H1 peptide	H2 peptide	H3 peptide
H <sub>2</sub> O	$\beta$ -structure	unordered	mostly unordered
increase in TFE (helix-promoting)	$\beta$ -structure	partially helical	partially helical
nonmicellar SDS ( $\beta$ -structure-promoting)	$\beta$ -structure	partially helical	$\beta$ -structure
micellar SDS (helix-promoting)	$\beta$ -structure	partially helical	partially helical

conformation depending upon its environment.<sup>41,70</sup> In many cases, the environment can override the propensity of a peptide to have a particular conformational preference if one can sufficiently vary the solvent medium, concentration, and temperature. In the case of hCG $\beta$ , we found that the three peptides studied, H1, H2, and H3, show different structural behavior even in the same environment. As summarized in Table 1, the H1 peptide has a strong intrinsic propensity to form a  $\beta$ -structure in several environments. This, coupled with its monomeric nature, makes it relatively unique and a potential model sequence for  $\beta$ -hairpin formation and  $\beta$ -sheet nucleation. The H3 peptide, studied earlier,<sup>32</sup> is more variable and undergoes transitions from an unordered structure to a  $\beta$ -like or  $\alpha$ -helix-like structure depending on the environment. By contrast, the H2 peptide, which adopts an unordered conformation in water, does not show any remarkable tendency for developing  $\beta$ -structure.

**hCG $\beta$  Folding Mechanism.** The variance in  $\beta$ -structure propensity for the three different hairpins should be accounted for in the folding mechanism of hCG $\beta$ . Previously, the kinetic folding pathway of hCG $\beta$  was studied using disulfide (S–S) bond formation as an index of folding. The order of S–S bond formation and the conversion of hCG $\beta$  folding intermediates was the same whether  $\beta$ -subunits fold intracellularly<sup>6–9</sup> or extracellularly (i.e., in vitro).<sup>81</sup> A framework-based model showing development of secondary and tertiary structure of hCG $\beta$  was proposed to fit the disulfide formation data.<sup>82</sup> This model assumed that the H1 and H3 antiparallel  $\beta$ -hairpins are formed autonomously at the earliest stages of the hCG $\beta$  folding and then H1 and H3 hydrophobically collapse to form a “molten globule” folding intermediate of this subunit.

Previous studies of peptide sequences derived from proteins have been used to shed light on the overall folding mechanism.<sup>10,74,83</sup> Structural propensities of peptides can be affected by environment, which is the rationale for varying solvent and concentration conditions, to learn relative folding propensities. With these caveats we suggest a revised mechanism for hCG $\beta$  based on the peptide studies presented above. The findings presented here are partially consistent with the previously proposed framework model. A combination of the framework and hydrophobic collapse models needs to be taken into consideration to describe a more detailed folding mechanism for hCG $\beta$  that is consistent with the data presented here. The H1 peptide adopts a  $\beta$ -structure in aqueous solution and has an unusual stability to solvent and concentration effects, indicating that it probably forms fast and thereby can act as an initiation site for hCG $\beta$  folding following a local framework mechanism. By contrast, the H3 peptide, as we had shown earlier,<sup>32</sup> can form a  $\beta$ -structure only under particular, partially hydrophobic

(63) Buchko, G. W.; Rozek, A.; Hoyt, D. W.; Cushley, R. J.; Kennedy, M. A. *Biochim. Biophys. Acta* **1998**, *1392*, 101–108.

(64) Lundahl, P.; Greijer, E.; Sandberg, M.; Cardell, S.; Eriksson, K. *Biochim. Biophys. Acta* **1986**, *873*, 20–26.

(65) Reynolds, J. A.; Tanford, C. *Proc. Natl. Acad. Sci. U.S.A.* **1970**, *66*, 1002–1007.

(66) Nelson, C. A. *J. Biol. Chem.* **1971**, *246*, 3895–3901.

(67) Takagi, T.; Tsujii, K.; Shirahama, K. *J. Biochem.* **1975**, *77*, 939–947.

(68) Everett, D. H. *Basic Principles of Colloid Science*; Royal Society of Chemistry: London, 1988.

(69) Jasanoff, A.; Fersht, A. R. *Biochemistry* **1994**, *33*, 2129–2135.

(70) Bruce, I. C.; Scott, R. P.; Fred, E. C. *Protein Sci.* **1993**, *2*, 2134–2145.

(71) Doty, P.; Holtzer, A. M.; Bradbury, J. H.; Blout, E. R. *J. Am. Chem. Soc.* **1954**, *76*, 4493.

(72) Liebes, L. F.; Zand, R.; Phillips, W. D. *Biochim. Biophys. Acta* **1975**, *405*, 27–39.

(73) Dyson, H. J.; Rance, M.; Houghten, R. A.; Wright, P. E.; Lerner, R. A. *J. Mol. Biol.* **1988**, *201*, 201–217.

(74) Shin, H. C.; Merutka, G.; Waltho, J. P.; Tennant, L. L.; Dyson, H. J.; Wright, P. E. *Biochemistry* **1993**, *32*, 6356–6364.

(75) Shiraki, K.; Nishikawa, K.; Goto, Y. *J. Mol. Biol.* **1995**, *245*, 180–194.

(76) Cox, J. P. L.; Evans, P. A.; Packman, L. C.; Williams, D. H. *J. Mol. Biol.* **1993**, *234*, 483–492.

(77) Blanco, F. J.; Serrano, L. *Eur. J. Biochem.* **1995**, *230*, 634–649.

(78) Blanco, F. J.; Jimenez, M. A.; Pineda, A.; Rico, M.; Santoro, J.; Nieto, J. L. *Biochemistry* **1994**, *33*, 6004–6014.

(79) Hollosi, M.; Majer, Z. S.; Ronai, A. Z.; Magyar, A.; Medzihradsky, K.; Holly, S.; Perczel, A.; Fasman, G. D. *Biopolymers* **1994**, *34*, 177–185.

(80) Vonstosch, A. G.; Jimenez, M. A.; Kinzel, V.; Reed, J. *Proteins: Struct., Funct., Genet.* **1995**, *23*, 196–203.

(81) Huth, J. R.; Perini, F.; Lockridge, O.; Bedows, E.; Ruddon, R. W. *J. Biol. Chem.* **1993**, *268*, 16472–16482.

(82) Ruddon, R. W.; Sherman, S. A.; Bedows, E. *Protein Sci.* **1996**, *5*, 1443–1452.

(83) Shin, H.; Merutka, G.; Waltho, J. P.; Wright, P. E.; Dyson, H. J. *Biochemistry* **1993**, *32*, 6348–6355.

environments. This suggests that the formation of the H3  $\beta$ -hairpin might be promoted to occur after a hydrophobic collapse (presumably between H1 and a region corresponding to the H3 fragment). The reduction in conformational space and consequent desolvation of the H3 region due to this collapse would then induce formation of the H3  $\beta$ -hairpin. The proposed mechanism of H3 formation is thus consistent with the hydrophobic collapse (rather than framework) model. Both the hydrophobic collapse and formation of H3 bring the termini of the H2 region into close proximity, which leads to stabilization of an H2 loop.

For the H2 peptide, our spectroscopic data do not show that the peptide has any remarkable tendency for developing  $\beta$ -structure even in environments known as  $\beta$ -structure-promoting. NMR data published earlier<sup>33</sup> clearly suggest that, in water, this peptide adopts an extended conformation containing a significant fraction of a PLPII-like structure. Our VCD data for the H2 peptide in water are consistent with such an interpretation, indicating stabilization of a significant fraction of a left-handed extended structure.<sup>38</sup> These observations all suggest that, in the process of the hCG $\beta$  folding, the H2 region would naturally form an extended loop, but could not initiate the folding.

In summary, the data presented here, when taken together, suggest that a framework-like mechanism describes the formation of hCG $\beta$  H1. However, a hydrophobic collapse model best describes subsequent events that occur as the subunit folds. This novel proposed combination of framework and hydrophobic collapse models, which helps clarify the hCG $\beta$  folding mechanism, is also consistent with X-ray data for mature, fully folded hCG.<sup>4,5</sup> Moreover, it is consistent with previous data describing the kinetic folding pathway of hCG $\beta$ <sup>6-9</sup> and suggests that a combined model may best define the folding pathway of this and, potentially, other proteins.

**Acknowledgment.** We thank Dr. Sam Sanderson from the Eppley Institute for synthesizing the H2 peptide used in our study. This work was supported, in part, by NIH Grant CA32949 to E.B. and an NCI Cancer Center Support Grant, P30CA 36727, to the Eppley Institute for Research in Cancer. Peptide conformational research in the UIC laboratory is supported in part by a grant from the donors of the Petroleum Research Fund, administered by the American Chemical Society.

JA0013172